Rational Design of Multiclade Coronavirus Spike Immunodominant Domain Nanoparticles Elicit Broad Antibody Responses

Christian K.O. Dzuvor[1], Sydney Moak[1,2], Lindsay R. McManus[1], Abigail Thomas[1,3], Abigail E. Dzordzorme[1,4,6], Taewoo Kim[1], Jeswin Joseph[1],Valerie Foley[1,3], Laura Novik[5], Ingelise J. Gordon[5], LaSonji A. Holman[5], Lesia K. Dropulic[5], Ryan P. McNamara[1], Kizzmekia S. Corbett-Helaire[1,2,7]

[1]Department of Immunology and Infectious Diseases; Harvard T.H. Chan School of Public Health; Boston, Massachusetts, 02115; United States of America

[2]Howard Hughes Medical Institute; Chevy Chase, Maryland, 20815; United States of America

[3]Northeastern University, Boston, Massachusetts, 02115; United States of America

[4]Harvard-MIT Division of Health Sciences and Technology, Institute for Medical Engineering and Science, Massachusetts Institute of Technology, Cambridge, Massachusetts, 02139; United States of America

[5]Vaccine Research Center; National Institutes of Allergy and Infectious Diseases; National Institutes of Health; Bethesda, Maryland, 20892; United States of America

[6]Current Affiliation: Wyss Institute for Biologically Inspired Engineering, Harvard University, Boston, Massachusetts,02215; United States of America

[7]Correspondance: kizzmekia_corbett@hsph.harvard.edu

Supplementary Figures

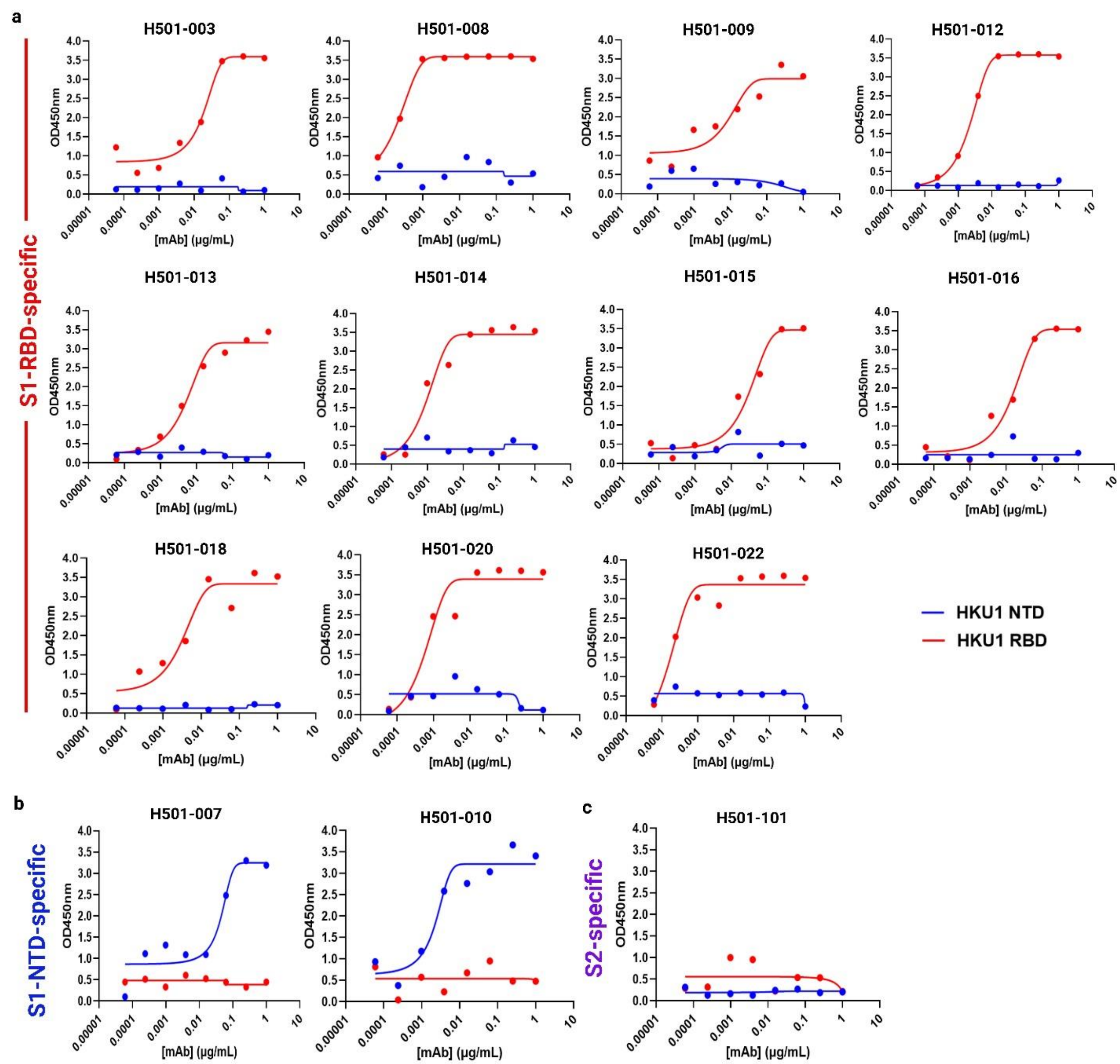

Supplementary Fig. 1: Antigenic characterization of hCoV-HKU1 S1 domain probes. (**a**) S1-RBD-specific mAbs, (**b**) S1-NTD-specific mAbs and (**c**) S2-specific mAb isolated from convalescent hCoV-HKU1-positive PBMCs were screened by ELISA for binding to HKU1 RBD (red) and HKU1 NTD (Blue) probes.

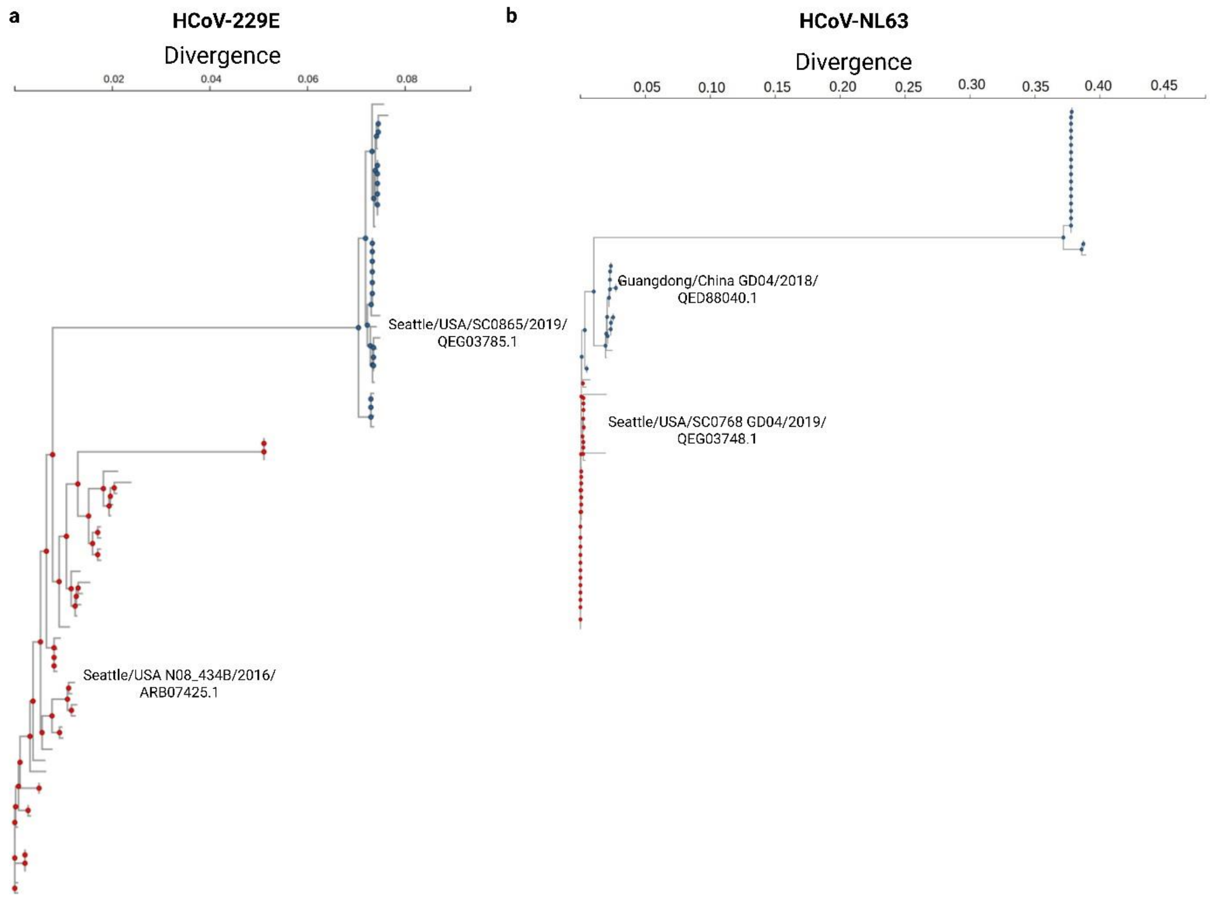
a
HCoV-229E
Divergence
0.02
0.04
0.06
0.08
Seattle/USA/SC0865/2019/
QEG03785.1
Seattle/USA N08_434B/2016/
ARB07425.1
b
HCoV-NL63
Divergence
0.05
0.10
0.15
0.20
0.25
0.30
0.35
0.40
0.45
Guangdong/China GD04/2018/
QED88040.1
Seattle/USA/SC0768 GD04/2019/
QEG03748.1

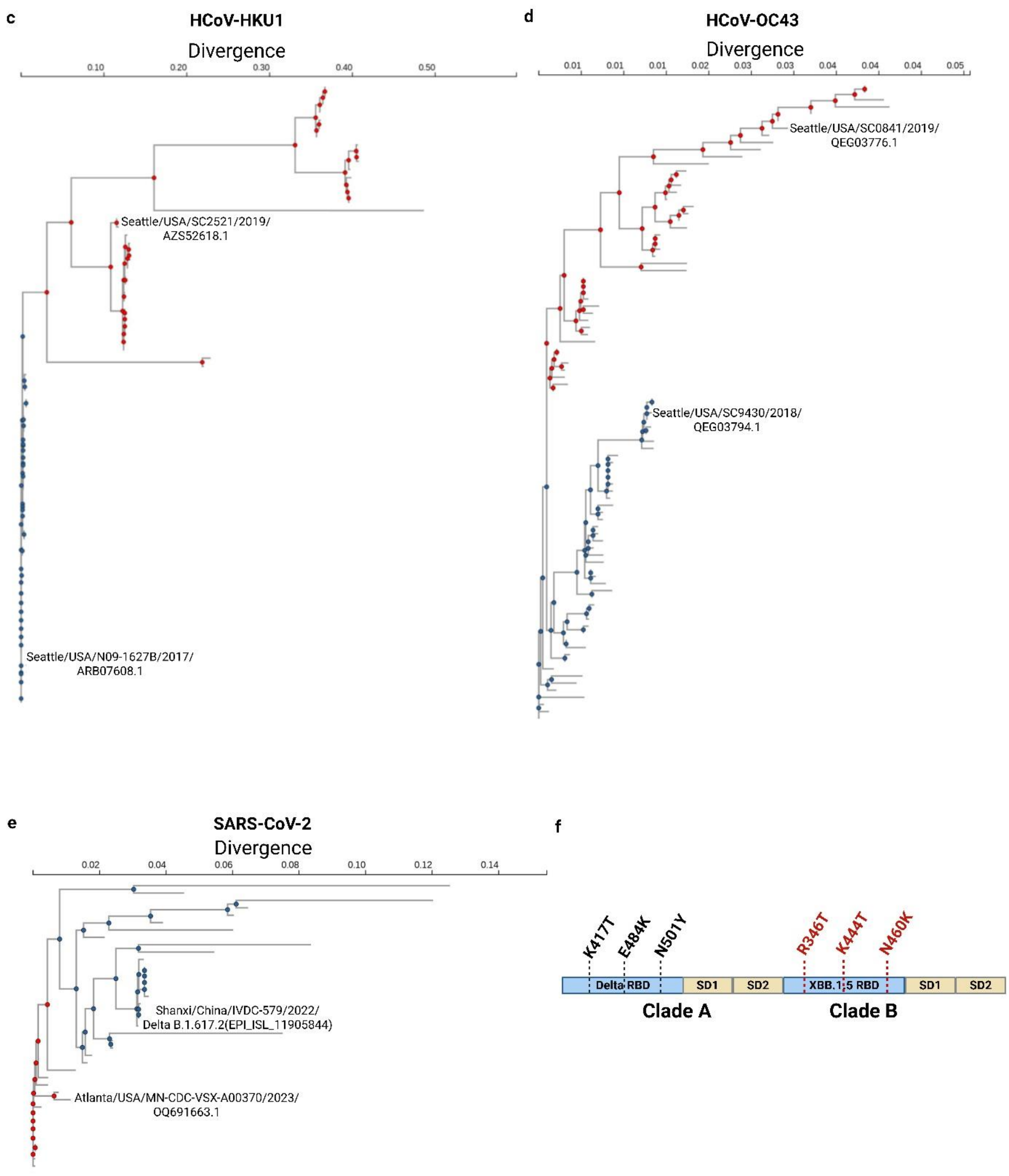

Supplementary Fig. 2: Selection of hCoV immunodominant domain (IDD) vaccine antigens, related to Fig. 1h. Spike Protein Sequences were identified using Nextstrain database and filtered by timeframe. (**a-e**) Phylogenetic trees were created with Clustal Omega EMBL-EBI using seeded guide trees and HMM profile-profile techniques and aligned by Clustal Omega MSA for HCoV (**a**) HCoV-229E, (**b**) HCoV-NL63 (**c**) HCoV-HKU1, (**d**) HCoV-OC43 and (**e**) SARS-CoV-2. Clades A and B are highlighted in blue and red, respectively. Selected S proteins for IDD vaccine designs are indicated. (**f**) Schematic depiction of mutation patches used to expand SARS-CoV-2 cross-variant antigenic coverage on the SARS-CoV-2 IDD construct.

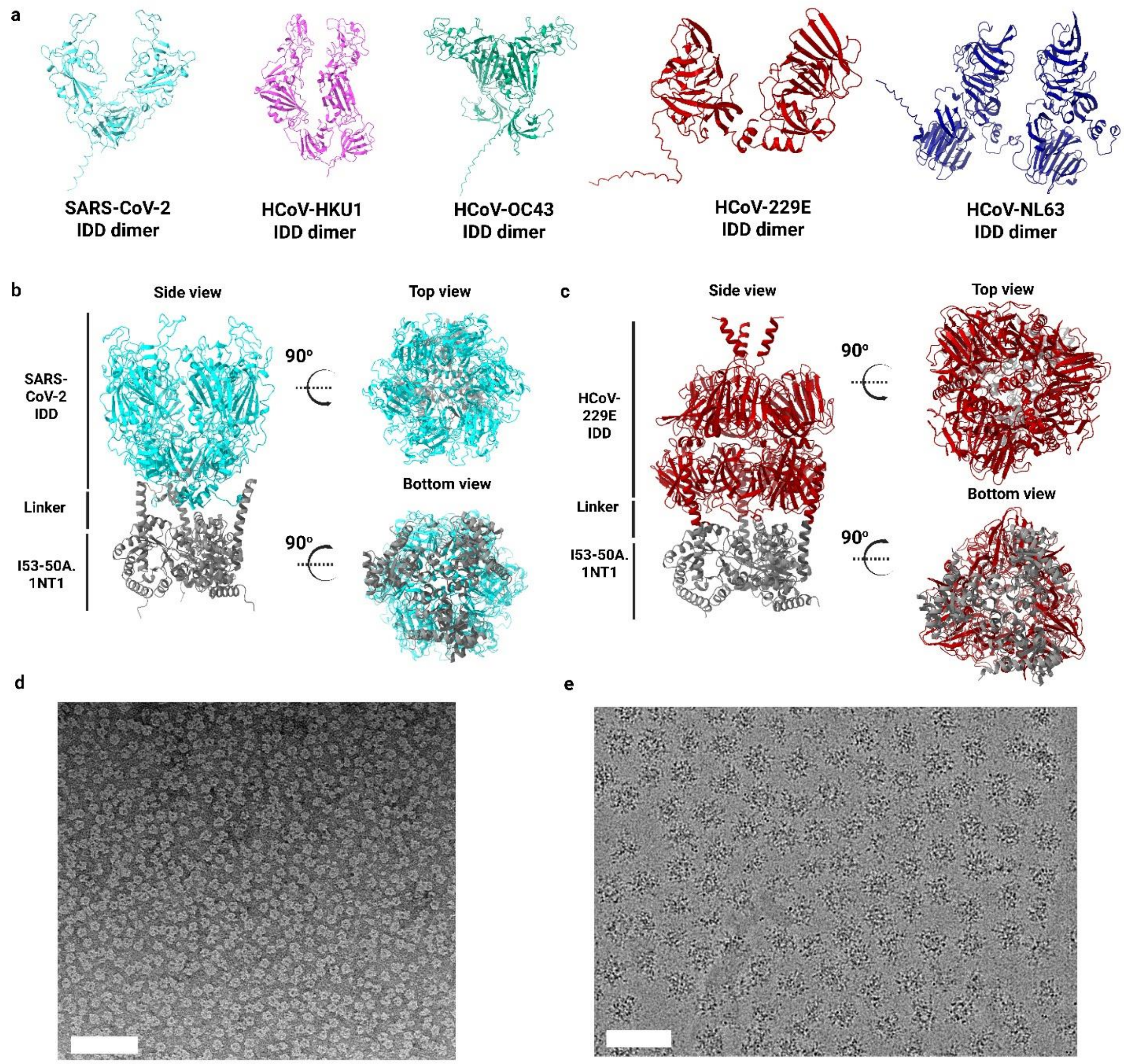

Supplementary Fig. 3: IDD design and NP characterization, related to Fig. 2. (**a**) AlphaFold structure prediction of monomeric chimeric IDD antigens. Molecular models of five HCoV IDDs. (**b-c**) Composite molecular models of chimeric immunodominant domain (IDD) trimers for representative endemic (**b**) β-HCoV (SARS-CoV-2) and (**c**) α-HCoV (HCoV-229E). The C-terminus of SARS-CoV-2 IDD (cyan) and HCoV-229E IDD (red) were fused to the N-termini of I53-50A trimer (gray) via a linker. (**d**) Representative negative-stain EM of purified bare I53-50 NP. Scale bar, 100 nm. (**e**) Representative cryo-EM micrograph of mosaic-5 IDD NP embedded in vitreous ice. Scale bar, 50 nm.

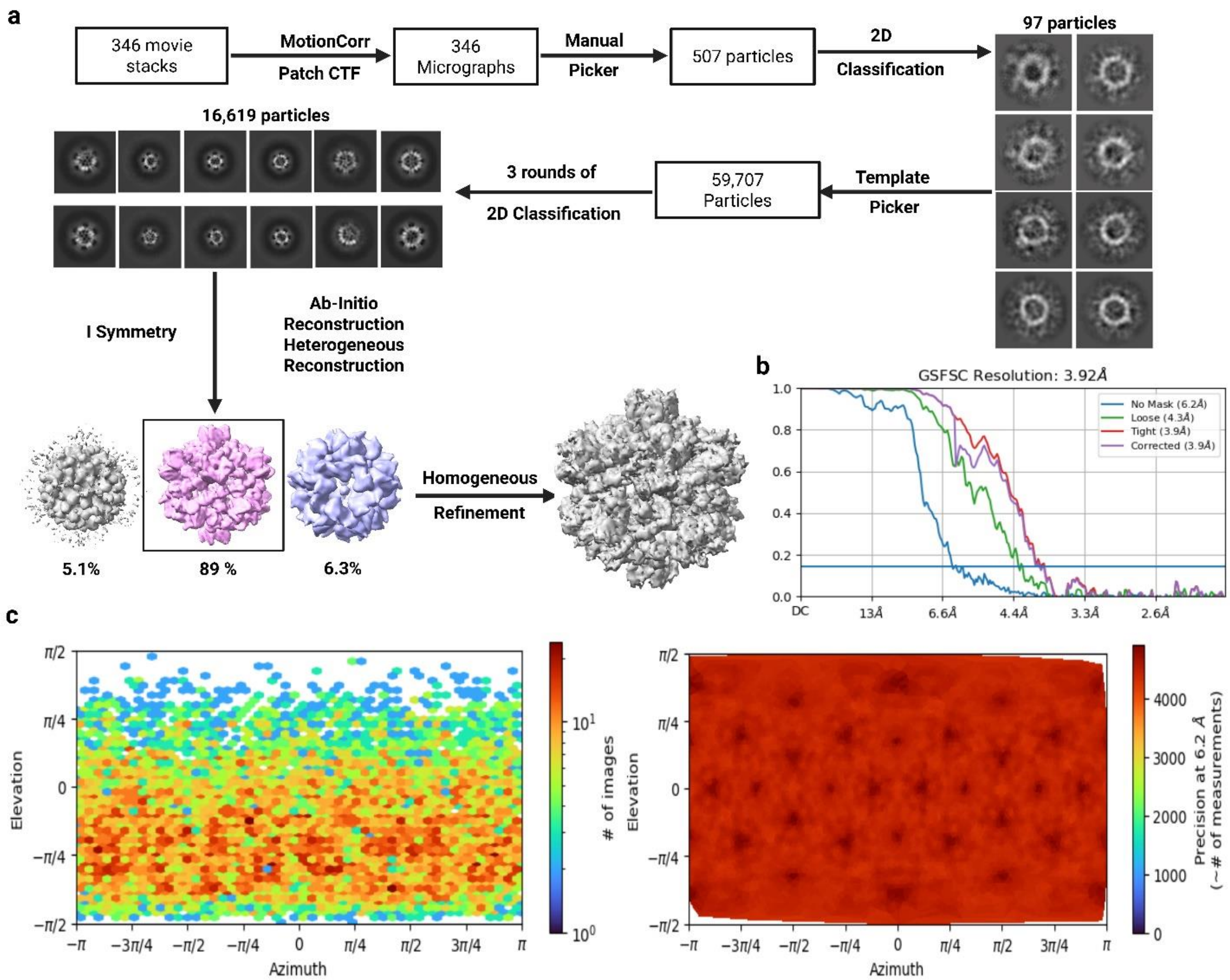

Supplementary Fig. 4: Cryo-EM structure determination of Mosaic-5 IDD NP, related to Figure 2D-E. (**a**) Cryo-EM data processing and reconstruction workflow showcasing all relevant and standard steps. 3D reconstruction was done using icosahedral symmetry. Final resolution was 3.9Å. (**b**) Gold-standard Fourier shell correlation (FSC) curve for the Mosaic-5 IDD NP density map shown in **Fig. 2e**. The 0.143 cut-off value is indicated by horizontal blue bar. (**c**) 2D Euler angular distribution plots used in reconstructions.

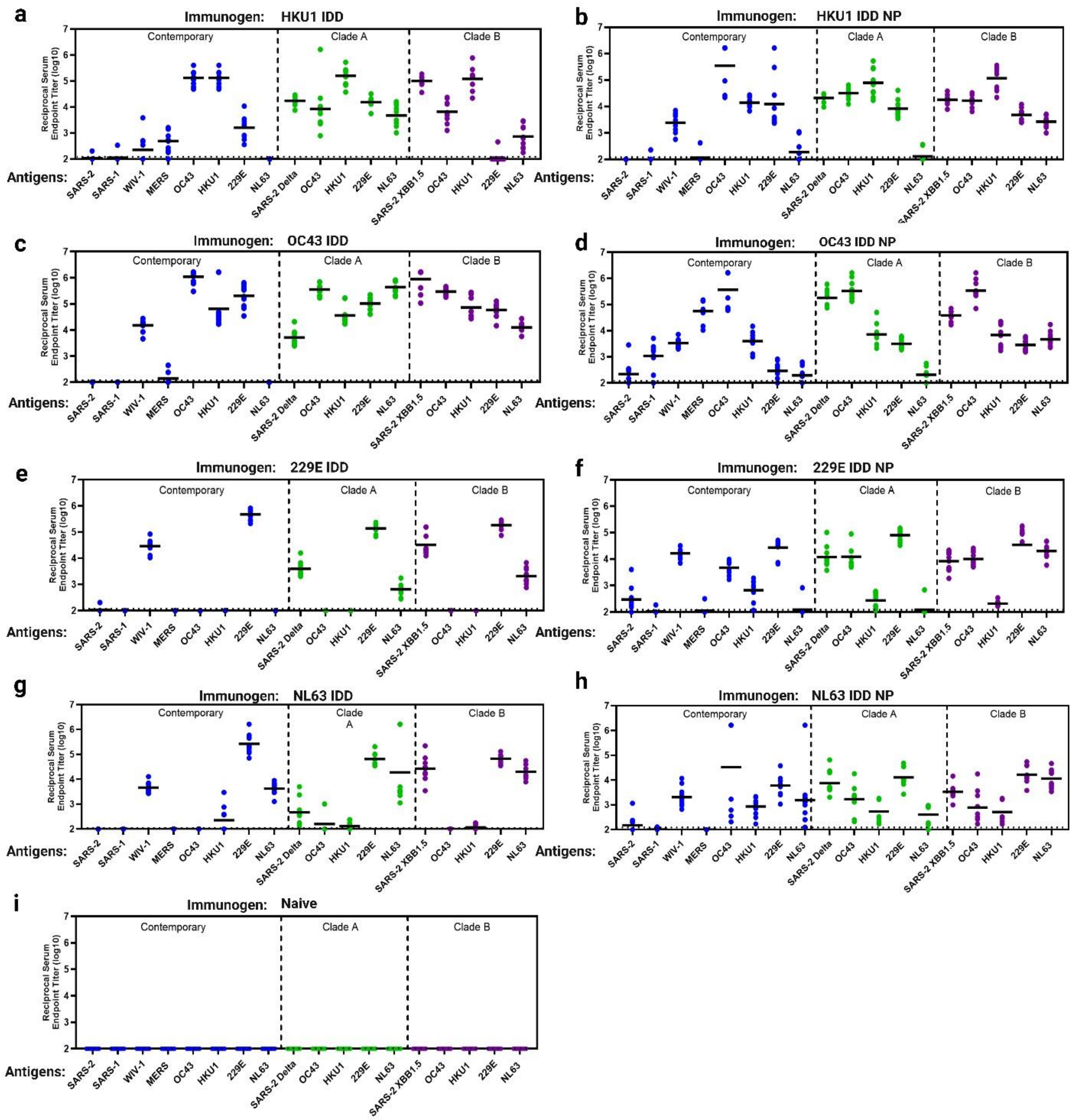

Supplementary Fig. 5: (a-i) Cross-reactive antibody responses in HCoV IDD and IDD NP immunized mice, related to Fig. 3. Female BALB/cJ mice (N = 10/group) were immunized at weeks 0 and 3 with 5 ug of IDD trimer (**a, c, e, g**) or IDD NPs (**b, d, f, h**) or Naive (**i**) with SAS adjuvant and bled at week 5 for serology. Control mice were immunized with adjuvanted PBS. Immune sera were assessed for antibody binding to various CoV S proteins by ELISA. Contemporary CoV S proteins are shown in blue. Clade A CoV S proteins are shown in green. Clade B CoV S proteins are shown in purple. Each dot represents an individual mouse. Horizontal dashed lines represent assay LOD.

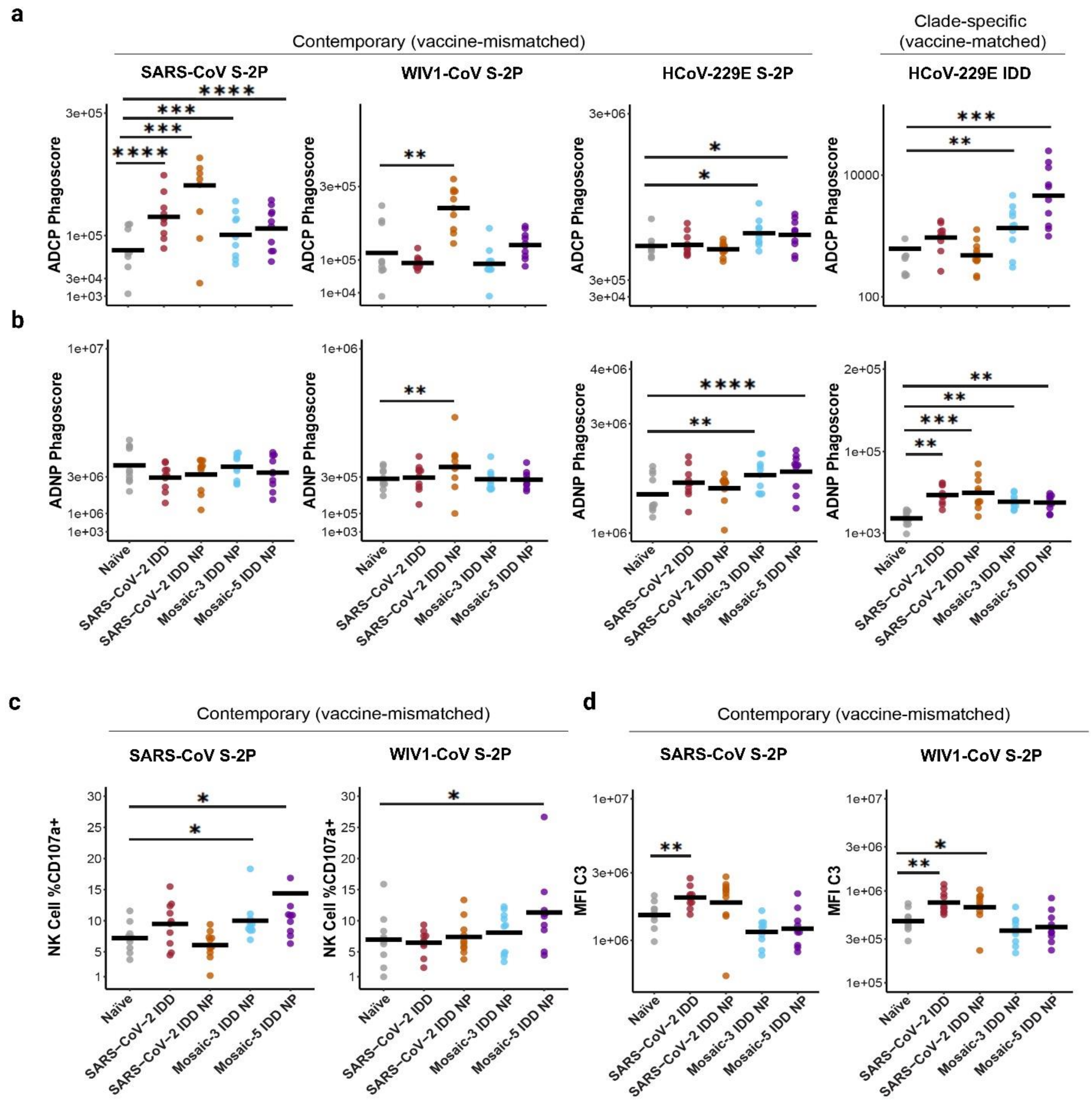

Supplementary Fig. 6: Antibody Fc-dependent functional scores (ADCP, ADNP, ADNK, ADCD) against pandemic threat and endemic coronavirus (HCoV-229E). (**a, b**) Fc-mediated effector functions of the naïve and immune sera after vaccination with IDD NPs against contemporary (SARS-CoV S-2P, WIV1-CoV S-2P, and HCoV-229E S-2P) and clade-specific (HCoV-229E IDD) protein. Antibody-mediated cellular phagocytosis with monocytes (ADCP, **a**) or neutrophils (ADNP, **b**) using IDD-vaccine-induced immune and naïve sera and beads coated with indicated SARS-CoV, WIV1-CoV, and HCoV-229E proteins. (**c**) Antibody-dependent natural killer cell activation (ADNKA) using IDD-vaccine-induced immune and naïve sera and beads coated with indicated SARS-CoV and WIV1-CoV S-2P proteins, as measured by the percentages of NK cells expressing CD107a against the antigens by vaccine group indicated. (**d**) Antibody-dependent complement deposition (ADCD) on beads coated with indicated SARS-CoV and WIV1-CoV S-2P proteins, and incubated with naïve or immune sera. In all figures, the horizontal black bar indicates the group mean value (N=10 mice per group). Each dot represents an individual mouse in a group. Two–way ANOVA with Tukey's post-hoc test was performed. The statistical significance is displayed as follows: $*p < 0.05$; $**p < 0.01$; $***p < 0.001$; $****p < 0.0001$. Source data file is provided.

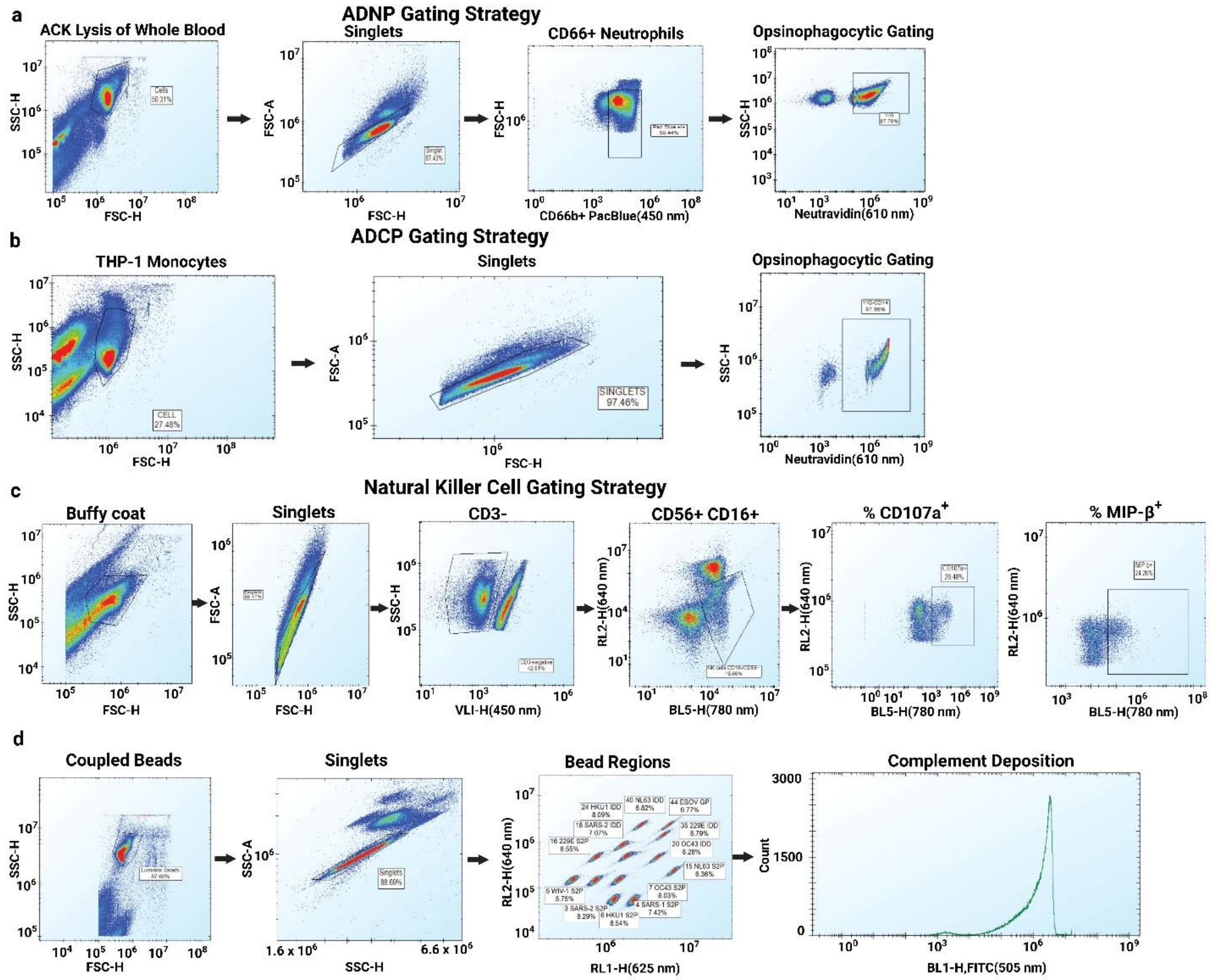

Supplementary Fig. 7: Flow cytometry gating strategy for Fc effector function assays, related to Fig. 5, Extended data Fig. 7 and Supplementary Fig. 6. (a) Gating for antibody-dependent neutrophil phagocytosis (ADNP) assay displaying CD66+ neutrophils with phagocytosed beads. (**b**) Gating for antibody-dependent cellular phagocytosis by monocytes (ADCP) assay displaying CD14+ monocytes with phagocytosed beads. (**c**) Gating for antibody-dependent natural killer cell activation (ADNKA) displaying CD56+/CD16-, and CD107a expression. (**d**) Gating for antibody-dependent complement deposition (ADCD) on CoV protein and antibody-coated beads.

Supplementary Tables

Supplementary Table. 1. HCoV convalescent donor information and sample details

VRC Study	Subject ID	Date of Confirmed CoV Infection	Sample Type	Blood Draw Information	
				Date	**Months after CoV[1]**
VRC 200	A	1/30/2014	PBMC	3/12/2014	1
VRC 500			Serum	2/10/2015	13
VRC 317	B	5/3/2018	Serum	7/11/2018	2
			PBMC		
	C	7/12/2018	Serum	10/4/2018	3
			PMBC		
	D	1/10/2018	Seum	4/12/2018	3
			PBMC		
VRC 200	E	3/20/2020	Serum	6/24/2020	3
			PBMC		

[1]Date of blood draw – Date of confirmed CoV infection)/12 = Months after CoV

Supplementary Table .2. Cryo-EM Data collection and processing parameters, related to Figure 2D-E.

Cryo-EM Data Collection and Processing Statistics	
EM Data Collection	
Microscope	Talos Arctica
Software	SerialEM
Voltage(kV)	200
Detector	Gatan K3
Magnification(Norminal)	36,000
Electron exposure(e-/ Å^2)	60.04
Defocus range (µm)	0.1-2.4
Pixel size(Å)	1.1
Flux (e-/pix/ Å)	12
Exposure time(seconds)	4.224
Total frames	47
Micrographs collected	346

3D Reconstruction Statistics	
Software	CryoSPARC v4.6.2
Symmetry imposed	I
Box size(pix)	450
Initial particle image no	346
Final particle image no	170
Map sharpening B-factor	-134
FSC threshold	0.143
Unmasked resolution at 0.143FSC(Å)	6.2
Masked resolution at 0.143FSC(Å)	3.9
Map resolution(Å)	3.92

Supplementary Table. 3: Sequences of designed immunogens and expression constructs reported in this study.

Construct Name	**Amino Acid Sequence**
Color Key	Secretion Signal Sequence, Clade A domain, Clade B domain, GS linker, Display Linker, I53-50A.1NT1, Streptag II, His-8-tag, I53-50B.4PT1
SARS-CoV-2 IDD-Linker-I53-50A.1NT1	MRGLGTCLATLAGLLLTAAGRFPNITNLCPFGEVFNATRFASVYAWNRKRISNCVADYSVLYNSASFSTFKCYGVSPTKLNDLCFTNVYADSFVIRGDEVRQIAPGQTGTIADYNYKLPDDFTGCVIAWNSNNLDSKVGGNYNYRYRLFRKSNLKPFERDISTEIYQAGSKPCNGVKGFNCYF PLQSYGFQPT YGVGYQPYRV VVLSFELLHA PATVCGPKKS TN LVKNKCVN FNFNGLTGTG VLTESNKKFL PFQQFGRDIADTTDAVRDPQTLEILDITPCSFGGGGSRFPNITNLCPFHEVFNATTFASVYAWNRKRISNCVADYSVIYNFAPFFAFKCYGVSPTKLNDLCFTNVYADSFVIRGNEVSQIAPGQTGNIADYNYKLPDDFTGCVIAWNSNKLDSTPSGNYNYRYRLFRKSKLKPFERDISTEIYQAGNKPCNGVA GPNCYSPLQS YGFRPTYGVG HQPYRVVVLS FELLHAPATV CGPKKSTNLVKNKCVNFNFNGLTGTGVLTE SNKKFLPFQQFGRDIADTTDAVRDPQTLEILDITPCSFGGGGGGSAEAAAKASSAEAAAKEAAAKEAAAKEEAARKMEELFKKHKIVAVLRANSVEEAIEKAVAVFAGGVHLIEITFTVPDADTVIKALSVLKEKGAIIGAGTVTSVEQCRKAVESGAEFIVSPHLDEEISQFCKEKGVFYMPGVMTPTELVKAMKLGHDILKLFPGEVVGPEFVKAMKGPFPNVKFVPTGGVDLDNVCEWFDAGVLAVGVGDALVEGDPDEVREKAKEFVEKIRGCTEGSLEWSHPQFEKGSGHHHHHHHH
HCoV-HKU1 IDD-Linker-I53-50A.1NT1	MDAMKRGLCCVLLLCGAVFVSPSASGSTVKPVATVHRRIPDLPDCDID KWLNNFNVPS PLNWERKIFS NCNFNLSTLL RLVHTDSFSCNNFDESKIYGSCFKSIVLDK FAIPNSRRSD LQLGSSGFLQ SSNYKIDTTS SSCQLYYSLP AINVTINNYN PSSWNRRYGF NNFNLSSHSVVYSRYCFSVNNTFCPCAKPSFASSCKSHKPPSASCPIGTNYRSCESTTVLDHTDWCRCSCLPDPITAYDPRSCSQKKSLVGVGEHCAGFGVDEEKCGVLDGSYNVSCLCSTDAFLGWSYDTCVSNNRCNIFSNFILNGINSGTTCSNDLLQPNTEVYTDVCVDYDLYGITGQGIFKEVSAVYYNSWQNLLYDSNGNIIGFKDFVTNKTYNIFPCYAGGGSTVKPVATVYRRIPNLPDCDIDNWLNNVSVPSPLNWERRIFSNCNFNLSTLLRLVHVDSFSCNNLDKSKIFGSCFNSITVDKFAIPNRRRDDLQLGSSGFLQSSNYKIDTTSSSCQLYYSLPAINVTINNYNPSSWNRRYGFNNFNLSSHSVVYSRYCFSVNNTFCPCAKPSFASSCKSHKPPSASCPIGTKYRHCDLDTTLYVKNWCRCSCLPDPISTYSPNTCPQKKVVVGIGEHCPGLGINEEKCGTQLNHSSCSCSPDAFLGWSFDSCISNNRCNIFSNFIFNGINSGTTCSNDLLYSNTDVSTGVCVNYDLYGITGQGIFKEVSAAYYNDWQNLLYDSNGNIIGFKDFLTNKTYTILPCYSGRVSGGGGSAEAAAKASSAEAAAKEAAAKEAAAKEEAARKMEELFKKHKIVAVLRANSVEEAIEKAVAVFAGGVHLIEITFTVPDADTVIKALSVLKEKGAIIGAGTVTSVEQCRKAVESGAEFIVSPHLDEEISQFCKEKGVFYMPGVMTPTELVKAMKLGHDILKLFPGEVVGPEFVKAMKGPFPNVKFVPTGGVDLDNVCEWFDAGVLAVGVGDALVEGDPDEVREKAKEFVEKIRGCTEGSLEWSHPQFEKGSGHHHHHHHH
HCoV-OC43 IDD-Linker-I53-50A.1NT1	MPMGSLQPLATLYLLGMLVASVLAIADVYRRKPDLPNCNIEAWLNDKSVPSPLNWERKTFSNCNFNMSSLMSFIQADSFTCNNIDAAKIYGMCFSSITIDKFAIPNRRKVDLQLGNLGYLQSSNYRIDTTATSCQLYYNLPAANVSVSRFNPSTWNKRFGFIEDAVFKPQPAGVLTNHDVVYAQHCFKAPKNFCPCSSCSGKNNGIGTCPAGTNSLTCDNLCTLDPITLKAPDTYKCPQSKSLVGIGEHCSGLAVKSDYCGNNSCTCQPQAFLGWSADSCLQGDKCNIFANFILHDVNNGLTCSTDLQKANTEIELGVCVNYDLYGISGQGIFVEVNATYYNSWQNLLYDSNGNLYGFRDYITNRTFMIHSCYSGGGSGVYELNGYTVQPIADVYRRKPDLPNCNIEAWLNDKSVPSPLNWERKTFSNCNFNMSSLMS

	FIQADSFTCNNIDAAKIYGMCFSSITIDKFAIPNGRKVDLQLGNLGYLQSFNYRIDTTATSCQLYYNLPAANVSVSRFNPSTWNKRFGFI EDSVFKPQPAGVLTDHDVVYAQHCFKAPKNFCPCKSNSSLCVGSGPGKNNGIGTCPAGTNYLTCHNLCNPDPITFTGPYKCPQTKSLV GIGEHCSGLAVKSDYCGGNPCTCQPQAFLGWSADSCLQGDKCNIFANLILHDVNSGLTCSTDLQKANTDIKLGVCVNYDLYGISGQGI FVEVNATYYNSWQNLLYDSNGNLYGFRDYITNRTFMIRSCYSGGGGSAEAAAKASSAEAAAKEAAAKEAAAKEEAARKMEELFKK HKIVAVLRANSVEEAIEKAVAVFAGGVHLIEITFTVPDADTVIKALSVLKEKGAIIGAGTVTSVEQCRKAVESGAEFIVSPHLDEEISQFC KEKGVFYMPGVMTPTELVKAMKLGHDILKLFPGEVVGPEFVKAMKGPFPNVKFVPTGGVDLDNVCEWFDAGVLAVGVGDALVEG DPDEVREKAKEFVEKIRGCTEGSLEWSHPQFEKGSGHHHHHHHH
HCoV-229E IDD -Linker-I53-50A.1NT1	MFVLLVAYALLHIAGCQTTNGTNTSHAVCNGCVGHSENVFAVESGGYIPSNFAFNNWFLLTNTSSVVDGVVRSFQPLLLNCLWSVSGSQ VITGFVYFNGTGRGACKGFYSNASSDVIRYNINFEENLRRGTILFKTSYGAVVFYCTNNTLVSGDAHIPSGTVLGNFYCFVNTTIGNETT SAFVGALPKTVREFVISRTGHFYINGYRYFSLGNVEAVNFNVTNAATTVCTVALASYADVLVNVSQTAIANIIYCNSVINRLRCDQLSGG SQTTNGMNTSHSVCNGCVGHSENVFAVESGGYIPSNFAFNNWFLLTNTSSVVDGVVRSFQPLLLNCLWSVSGSRLTTGFVYFNGTGRG DCKGFYSNASSDVIRYNINFEENLRRGTILFKTSYGAVVFYCTNNTLVSGDAHIPSGTVLGNFYCFVNTTIGNETTSAFVGALPKTVREF VISRTGHFYINGYRYFSLGNVEAVNFNVTNAATTVCTVALASYADVLVNVSQTAIANIIYCNSVINRLRCDQLSGGGGSAEAAAKASSA EAAAKEAAAKEAAAKEEAARKMEELFKKHKIVAVLRANSVEEAIEKAVAVFAGGVHLIEITFTVPDADTVIKALSVLKEKGAIIGAGTV TSVEQCRKAVESGAEFIVSPHLDEEISQFCKEKGVFYMPGVMTPTELVKAMKLGHDILKLFPGEVVGPEFVKAMKGPFPNVKFVPTGG VDLDNVCEWFDAGVLAVGVGDALVEG DPDEVREKAKEFVEKIRGCTEGSLEWSHPQFEKGSGHHHHHHHH
HCoV-NL63 IDD-Linker-I53-50A.1NT1	MKLFLILLILPLVSCFSTCNSNASISMLQLGVPDNSSTIVTGLLPVHWICANQSTSTYPANGFFYIDVGKHRSAFALHSG YYDANQYYIY LTNNISLNAPVTLKICKFGNTSFACLSNVSTSHHCIVNSSFTEQLGVPLGITISGETVRLHLYNATRTFYVPAAYKLTKLSVKCYFSESC VFSVVNATVTVNVTTLNGRIVNYTVCDDCNGYTDNIFSVQQDGRIPNGFSFNNWFLLTNGSTLVDGVSRLYQPLRLTCLWPVPGLKSS TGFVYFNATGSDVNCNGYQHHSVADVMRYNLNFSSNSVDNLKSGVIVFKTLQYDVLFYCSNSSSGVLDTTIPFGPSSQPYYCFINSTIN TTHVSTFVGVLPPIVREIVVARTGQFYINGFKYFDLGFIEAVNFNVTTASATDFWTVAFATFVDVLVNVSATNIQNLLYCDSPFEKLQC EHLQFGLQDGFYSANFLDDNVLPD**GGS**SNANLSMLQLGVPDNSSTIVTGLLPTHWICANQSTSVYSANGFFFIDVGNHRSAFALHTG YYDVNQYYIYVTNEIGLNASVTLKICKFGNTTFDFLSNSSSSFDCIVNLLFTEQLGAPLGITISGETVRLHLYNVTRTFYVPAAYKLTKL SVKCYFNYSCVFSVVNATVTVNVTTHNGRVVNYTVCDDCNGYTDNIFSVQQDGRIPNGFPFNNWFLLTNGSTLVDGVSRLYQPLRLT CLWPVPGLKSSTGFVYFNATGSDVNCNGYQHNSVADVMRYNLNFSANSVDNLKSGVIVFKTLQYDVLFYCSNSSSGVLDTTIPFGPSS QPYYCFINSTINTTHVSTFVGVLPPTVREIVVARTGQFYINGFKYFDLGFIEAVNFNVTTASATDFWTVAFATFVDVLVNVSATKIQNLL YCDSPFEKLQCEHLQFGLQDGFYSANFLDDNGGGGSAEAAAKASSAEAAAKEAAAKEAAAKEEAARKMEELFKKHKIVAVLRANS VEEAIEKAVAVFAGGVHLIEITFTVPDADTVIKALSVLKEKGAIIGAGTVTSVEQCRKAVESGAEFIVSPHLDEEISQFCKEKGVFYMPG VMTPTELVKAMKLGHDILKLFPGEVVGPEFVKAMKGPFPNVKFVPTGGVDLDNVCEWFDAGVLAVGVGDALVEGDPDEVREKAKE FVEKIRGCTEGSLEWSHPQFEKGSGHHHHHHHH
I53-50A.1NT1	MKMEELFKKHKIVAVLRANSVEEAIEKAVAVFAGGVHLIEITFTVPDADTVIKALSVLKEKGAIIGAGTVTSVEQCRKAVESGAEFIVS PHLDEEISQFCKEKGVFYMPGVMTPTELVKAMKLGHDILKLFPGEVVGPEFVKAMKGPFPNVKFVPTGGVDLDNVCEWFDAGVLAV GVGDALVEG DPDEVREKAKEFVEKIRGCTEGSLEHHHHHHHH
I53-50B.4PT1	MNQHSHKDHETVRIAVVRARWHAEIVDACVSAFEAAMRDIGGDRFAVDVFDVPGAYEIPLHARTLAETGRYGAVLGTAFVVNGGIY RHEFVASAVINGMMNVQLNTGVPVLSAVLTPHNYDKSKAHTLLFLALFAVKGMEAARACVEILAAREKIAAGSLEHHHHHHHH